Effect of interface configurations on the dynamic scaling behavior of Pb(Zr0.53Ti0.47)O3 thin films

Kui Li, Nossikpendou Sama, Tao Li, Denis Remiens, Gang Du, Xianlin Dong, Genshui Wang

Applied Physics Letters

Effect of interface configurations on the dynamic scaling behavior of $Pb(Zr_{0.53}Ti_{0.47})O_3$ thin films

Cite as: Appl. Phys. Lett. **104**, 092904 (2014); https://doi.org/10.1063/1.4867506
Submitted: 22 December 2013 • Accepted: 21 February 2014 • Published Online: 05 March 2014

Kui Li, Nossikpendou Sama, Tao Li, et al.

Effect of interface configurations on the dynamic scaling behavior of $Pb(Zr_{0.53}Ti_{0.47})O_3$ thin films

Kui Li,[1,2,3] Nossikpendou Sama,[3] Tao Li,[1] Denis Rémiens,[3] Gang Du,[1] Xianlin Dong,[1] and Genshui Wang[1,a)]

[1]*Key Laboratory of Inorganic Functional Materials and Devices, Shanghai Institute of Ceramics, Chinese Academy of Sciences, 1295 Dingxi Road, Shanghai 200050, People's Republic of China*
[2]*Jiangsu Key Laboratory of Biofunctional Materials, College of Chemistry and Materials Science, Nanjing Normal University, Nanjing 210023, People's Republic of China*
[3]*Institute of Electronics, Microelectronics and Nanotechnology (IEMN)—DOAE, UMR CNRS 8520, Université de Valenciennes et du Hainaut Cambrèsis Valenciennes 59313 Cedex, France*

(Received 22 December 2013; accepted 21 February 2014; published online 5 March 2014)

The ferroelectric hysteresis and the scaling relations of hysteresis area $\langle A \rangle$ against field amplitude E and frequency f in $Pb(Zr_{0.53}Ti_{0.47})O_3$ thin films using platinum and $LaNiO_3$ (LNO) as both bottom and top electrodes were systematically investigated. Interestingly, it was found that the influence of top electrodes is dominant in affecting the scaling behavior of the dynamic hysteresis, which may be the result of the asymmetric interface structure deriving from the differences in conductivity and crystallization of the top and bottom LNO electrodes. The bottom electrodes affect the scaling behavior slightly via influencing the micro-structural and level of space charge. © *2014 AIP Publishing LLC*. [http://dx.doi.org/10.1063/1.4867506]

Considering their superior ferroelectric and piezoelectric properties, lead zirconate titanate (PZT) thin films have been extensively investigated for applications in nonvolatile random access memory devices. The problem of dynamic hysteresis, disclosed by a so-called scaling power law, is of special importance for this application since the dynamic response of hysteresis can provide a lot of critical information from both academic and commercial viewpoints.[1–3] The power law of $\langle A \rangle \propto f^{\alpha}E^{\beta}$ (where $\langle A \rangle$ is hysteresis area, E is the amplitude of electric field, f is frequency, and α as well as β are scaling exponents that depend on the dimensionality and symmetry of the system) have been conducted theoretically for ferromagnetic and ferroelectric by Rao *et al.* and the scaling exponents α and β were -1 and 2, respectively, in terms of the three-dimensional $(\Phi^2)^2$ and $(\Phi^2)^3$ models.[4] However, there is dramatically variance for the exponent values derived from some experimental investigations carried out in both bulk ceramics and thin films to that from theoretical predictions[4–12] (as listed in Table I). Moreover, unlike their bulk counterparts, ferroelectric thin films are normally grown on substrate and the electrodes are prepared on both sides of the ferroelectric thin films to form the capacitor structure, which brings the thin films extra stress and interface effect. Consequently, a significant amount of research has been devoted to understand the effects of the interface structure on the ferroelectric and fatigue properties in PZT thin films over the past years. The interface effect may explain the different dynamic scaling behavior of the thin films with different electrode configurations. It has been extensively reported that the interface structure dramatically affects the properties, including the ferroelectric hysteresis, of PZT thin films because of their different built-in electric field,[13] imprinted polarization,[14] Schottky contact barrier,[15] charge accumulation and injection near the electrode interface and interface ferroelectricity.[16] Unfortunately, the effect of interface structure as well as the electrode configuration on the dynamic scaling behavior was rarely investigated in the thin films prepared with different top and bottom electrodes. It is thus the aim of the present investigation to experimentally study the effect of both top and bottom electrodes on the dynamic hysteresis behavior for the $Pb(Zr_{0.53}Ti_{0.47})O_3$ thin films with different capacitor structures of Pt/PZT/Pt/Si, LNO/PZT/Pt/Si, LNO/PZT/LNO/Si, and Pt/PZT/LNO/Si.

Silicon substrate is coated with SiO_2 (3000 Å) passivation layer and a thin TiO_x (10 nm) layer is deposited between SiO_2 and Pt bottom electrode. The LNO bottom electrode which was *in situ* deposited on SiO_2/Si at 450 °C and post-annealed at 700 °C in air like Pt bottom electrode,[21] which improves the crystallization and interface structure between PZT and both Pt and LNO bottom electrodes. $Pb(Zr_{0.53}Ti_{0.47})O_3$ thin films with a thickness of 960 nm were deposited by r.f. magnetron sputtering method with a r.f. power density of 2.36 W/cm^2 under a pressure of 10^{-2} millibars in argon atmosphere. The films were deposited without heating substrate, and post-annealing process at 625 °C for 1 h was adopted to transform the films from amorphous to perovskite phase. The detailed information of the preparation of PZT thin films was introduced elsewhere.[17] Both Pt and LNO top electrodes with a diameter of 150 μm were fabricated via magnetron sputtering method to form the different capacitor structures of Pt/PZT/Pt/Si, LNO/PZT/Pt/Si, LNO/PZT/LNO/Si, and Pt/PZT/LNO/Si (denoted as S1, S2, S3, and S4, respectively). The polarization-electric field (P-E) hysteresis loops at various frequency (f) ranging from 1 Hz to 1 kHz and field amplitude (E) values varying from 40 kV/cm to 240 kV/cm at room temperature were measured using an aixACT TF 2000 analyzer (aixACT Systems GmbH, Aachen, Germany). The hysteresis loop area $\langle A \rangle$ was calculated by integrating the area bounded by the P-E

a)Electronic mail: genshuiwang@mail.sic.ac.cn

TABLE I. Dynamic scaling exponents for different systems.

System	α	β	References
$(\Phi^2)^2$ and $(\Phi^2)^3$ models	−1	2	4
$YBa_2Cu_3O_7$ (YBCO)/PZT/YBCO high f	−1/3	1	5
Low f	1/3	2/3	
Pt/$SrBi_2Ta_2O_9$/Pt high f	−1/3	2	6
Low f	2/3	2/3	
Hard PZT low E	−0.43	3.19	8
Bulk ceramic high E	−0.28	0.89	
Soft PZT low E	−1/3	3	9
Bulk ceramic high E	−0.25	1	

loops. The crystal quality and micro-structure of the PZT thin films with different electrode configurations were investigated by X-ray diffraction (XRD) analysis (Siemens D5000 diffractometer) and scanning electronic microscope (SEM) Hitachi S4700 (Hitachi, États-Unis, TX).

Unlike LNO bottom electrodes, LNO top electrodes were deposited without heating the substrate and annealed at much lower temperature of 500 °C, which is enough for the Pt metal top electrode while insufficient for crystallization quality and conductivity improvement of LNO top electrode. Figure 1 shows structural properties of LNO electrodes (top and bottom). As shown in Fig. 1(a) and its inset, the LNO bottom electrode is highly (100)-orientated and grain size less than 100 nm has resistivity of 4.5×10^{-6} Ω/m, whereas LNO top electrode is randomly oriented with grain size more than 100 nm and resistivity of 8×10^{-6} Ω/m. As demonstrated in Fig. 1(b), whatever the bottom electrode, PZT thin film is pure perovskite phase without any second peaks such as parasitic pyrochlore phase. However, the PZT film deposited on LNO bottom electrode is (100)-orientated, while the one on Pt electrode shows random orientation. Figs. 1(c) and 1(d) show STEM images of PZT/Pt/Si and PZT/LNO/Si films, respectively. The PZT thin film deposited on LNO bottom electrode possesses grain size ranging from 80 to 200 nm, whereas the film on Pt bottom electrode shows bulk-like grains larger than 1 μm. The cross-section samples with all four kinds of electrodes configuration were obtained by FIB method, observed by STEM and analyzed by Energy Dispersive X-ray (EDX). As exhibited by the insets of Figs. 1(c) and 1(d), the use of LNO as bottom electrode is of great advantage in terms of diffusion barrier. Indeed, the interface between PZT and bottom LNO is very smooth and sharp whereas there is an inter-diffusion zone between bottom Pt and PZT. A thin Pb-Pt type intermetallic layer with a thickness of about 20 nm was determined between Pt bottom electrode and PZT layer. Also into the Pt bottom electrode, ~3% (atomic concentration) of Pb atoms was present. The diffusion of Pb is exacerbated by heat treatments and no diffusion was found either between PZT and Pt top electrode or between PZT and LNO. Interestingly, previous works devoted to size effect and ferroelectric fatigue in PZT thin films revealed that the nature of top electrode had dominated influence in terms of dielectric and electrostatic properties of the whole interface (including both top and bottom interfaces) which were determined as key factors in size effect and ferroelectric fatigue.[23] The results of these experimental and modeling studies revealed that considering the serial capacitance model, LNO top electrode promotes a relatively high and charge-free interface capacitance whereas Pt top electrode induces a low interface capacitance with a built-in potential.

The polarization–electric field (P–E) loops of PZT thin films with different electrode configurations were presented in Fig. 2. The different interface structure affects the ferroelectric properties dramatically in terms of coercive field E_c. It is clearly noticeable that top electrode is dominant factor in influencing the ferroelectric properties. Whatever the nature of bottom electrode (Pt or LNO), the thin films show much lower coercive field when LNO is adopted as top electrode as shown in the inset (a) of Fig. 2. The P-E loops of PZT thin films show drastically different asymmetry with regard to residual polarization P_r and coercive field E_c for the different capacitor configurations. As shown in the inset (b) of Fig. 2, PZT thin films with LNO top electrode which suffered different processing temperature from that of

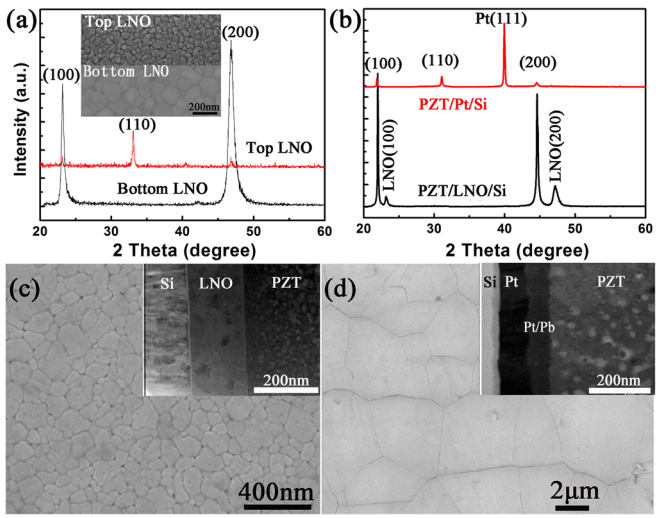

FIG. 1. The XRD patterns of (a) the LNO electrode and (b) the PZT thin films deposited on different bottom electrodes, inset in Fig. 1(a) shows the surface morphologies of LNO bottom electrodes. Surface and cross-section (insets) SEM photographs of the PZT thin films deposited on (c) LNO and (d) Pt bottom electrode.

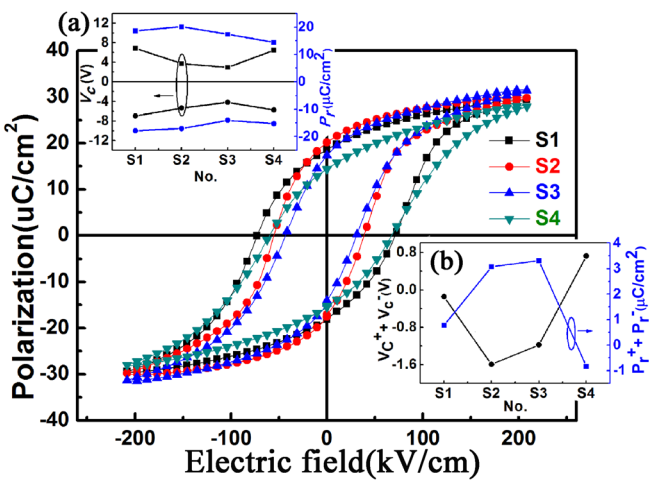

FIG. 2. Polarization loops of 960 nm thickness PZT films with different interface configurations. The insets show (a) values and the (b) asymmetry of coercive field and residual polarization of the films with different electrode configurations, respectively.

bottom electrode[18] demonstrate larger dissymmetry for both residual polarization P_r and coercive field E_c no matter what kind of bottom electrode is adopted and the orientation of the films, which may be stemmed from the different internal bias field and depolarization field due to asymmetric carrier compensation.[19,20] These results imply that the interface structure between top electrode and the PZT thin films is a very important factor in influencing the ferroelectric properties of the films.[18]

Fig. 3 shows the evolution of dynamic hysteresis area ⟨A⟩ as a function of frequency f in PZT thin films with different capacitor structures at electric fields of (a) 40 kV/cm and (b) 200 kV/cm. Interestingly, it is found that the hysteresis area shows different evolutions with both the electric field amplitude and capacitor configurations. As shown in Fig. 3(a), the dynamic hysteresis area ⟨A⟩ monotonously decreases for all the films with increasing frequency (f) because parts of domain reversal cannot catch up with the varying of electric field and hence the consumed energy decreases, while hysteresis area ⟨A⟩ of the films with LNO as top electrodes is larger, which may be attributed to their lower coercive field than that of the films with Pt as top electrode as indicated in the ferroelectric analysis so that the larger number of nucleation and reversal domains. Moreover, hysteresis area ⟨A⟩ of the films with top electrodes of LNO decreases more slowly with frequency. For the films with LNO as top electrodes, the number of nucleation domains is much larger because of their lower coercive field which makes the domain reversal easier, and hence the energy consuming of the domain reversal (i.e., ⟨A⟩) decreases.[22] The dynamic hysteresis area as a function of frequency for the films with saturated loops at 20 V is demonstrated in Fig. 3(b). The hysteresis area ⟨A⟩ of the films with top electrodes of Pt show monotonous increasing trend with frequency increasing from 1 Hz to 1 kHz and similar scaling exponents to that reported by Zhang in $0.67Pb(Mg_{1/3}Nb_{2/3})O_3$–$0.33PbTiO_3$ (PMN-PT) bulk ceramics,[22] which may be stemmed from their symmetrical interface effect on the dynamic hysteresis loops and thus analogous behavior in comparison to the bulk material as testified in the ferroelectric analysis. Strangely, PZT thin films with LNO top electrodes show different evolution of dynamic hysteresis area against the frequency, that is the area ⟨A⟩ first decreases rapidly while then decays more slowly with further increasing frequency. Compared with the scaling behavior of PZT thin films with Pt as top electrodes, these different behaviors may be attributed to the competition between the period of field (f^{-1}) and the time of domain reversal (τ) because of the poor crystallization of LNO top electrodes and potential ohmic nature of the interface structure between the PZT film and LNO top electrode, while Schottky type between PZT and Pt top electrode. The different interface structures between PZT and bottom electrode in the films with top LNO electrode show weak effect on the dynamic hysteresis behavior in the frequency ranging from 1 Hz to 1 KHz via influencing the different micro-structure and orientation of the films.

Fig. 4 shows the scaling behavior of hysteresis area ⟨A⟩ as a function of electric field E in the PZT thin films possessing different capacitor structures with a fixing frequency of 1 kHz at electric fields ranging from 40 to 250 kV/cm. Two perfect linear relations were identified for PZT thin films with Pt as top electrodes. The dynamic hysteresis area first

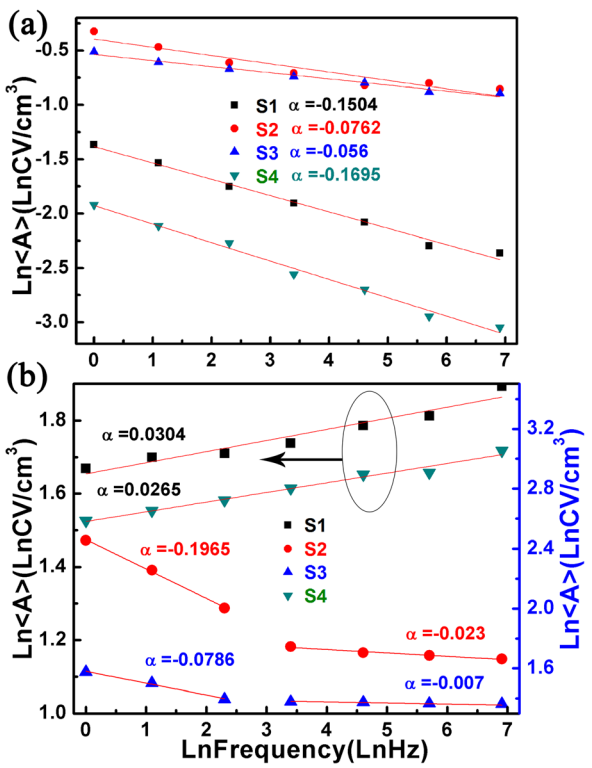

FIG. 3. The hysteresis area ⟨A⟩ as a function of frequency f of the films with different interface configurations tested at (a) 4 V and (b) 20 V.

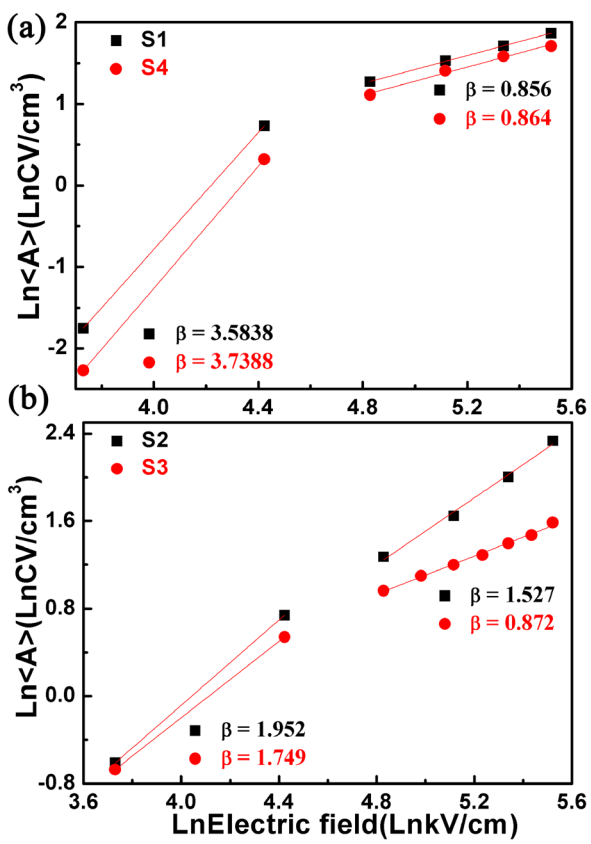

FIG. 4. The hysteresis area ⟨A⟩ as a function of electric field E of the films with (a) Pt and (b) LNO as top electrodes.

increases very rapidly at lower electric field than 83 kV/cm, which is very near to their coercive electric field, and then increases more slowly with further increased electric field. These results reveal that the mass ferroelectric domains can be easily reversed under low electric field, while defect and space charge accumulated at the interface between Pt top electrode and PZT films[23] may clamp domains and increase the electric field to switch the domains. At the same time, the exponent β values representing the ability of domains following the electric field direction were determined to be (3.584, 0.856) and (3.74, 0.865) in the films with Pt and LNO as bottom electrodes for these two stages, respectively. Moreover, the exponents of the scaling relations at both low and high electric field are very close to those in hard, soft PZT and PMNT ceramics,[8,9,22] which further validate the assumption proposed in the analysis of hysteresis area $\langle A \rangle$ against frequency. Similar to the trend observed in last part, the films with LNO top electrode show different evolution of hysteresis area as a function of electric field in that the area $\langle A \rangle$ increases monotonously with the electric field increasing from 40 kV/cm to 250 kV/cm, which may be the result of the less space charge and defect accumulation in the interface between LNO and PZT films. The slightly difference in the scaling exponents may be due to the different crystallographic anisotropy of the films prepared on different bottom electrodes. The PZT films deposited on LNO and Pt bottom electrodes are (100) and randomly oriented and the domain reversal in the former may be more difficult.[23]

To quantitatively descript the effect of the electrode configurations on the dynamic hysteresis of the thin films, we investigate the scaling behaviors of $\langle A \rangle$ against E, f. Based on the data analyzed above, the fitting results are shown in Fig. 5 for the films possessing different electrode configurations with saturated loops and the dynamic scaling behavior can be described by the following relations within the measured uncertainty:

$$\langle A \rangle \propto f^{0.0304} E^{0.856} \text{ for S1}, \quad \langle A \rangle \propto f^{-0.023} E^{1.527} \text{ for S2},$$
$$\langle A \rangle \propto f^{-0.007} E^{0.872} \text{ for S3}, \quad \langle A \rangle \propto f^{0.0265} E^{0.864} \text{ for S4}. \tag{1}$$

Interestingly, the films with Pt as top electrodes (S1 and S4) show similar scaling exponents of α and β, while the films with LNO as top electrodes (S2 and S3) exhibit analogical scaling behavior. These results indicate that the bottom electrode and the orientation of the PZT thin films don't affect the dynamic scaling behavior dramatically while the top electrodes as well as interface between them and PZT thin films are the major factors in affecting the scaling behavior, which can be attributed to the different conductivity and crystallization of the Pt and LNO top electrodes post annealed at 500 °C. Moreover, the scaling exponents change slightly with different kind of bottom electrodes for the films for a given top electrode (LNO or Pt), which may be the result of the different orientation of the thin films and the different level of space charge.

$Pb(Zr_{0.53}Ti_{0.47})O_3$ thin films using platinum and LNO as both bottom and top electrodes were deposited via magnetron sputtering method. The ferroelectric hysteresis and the scaling relations of hysteresis area $\langle A \rangle$ against frequency f and field amplitude E for the saturated loops in these capacitors and the effects of top as well as bottom electrodes on these properties were investigated systematically. Interestingly, it was found that the influence of top electrodes is dominant compared to the bottom electrodes in affecting the scaling behavior of the dynamic hysteresis, which may be attributed to the different conductivity and crystallization of the different top electrodes annealed at the same while much lower temperature than that of bottom electrodes. The

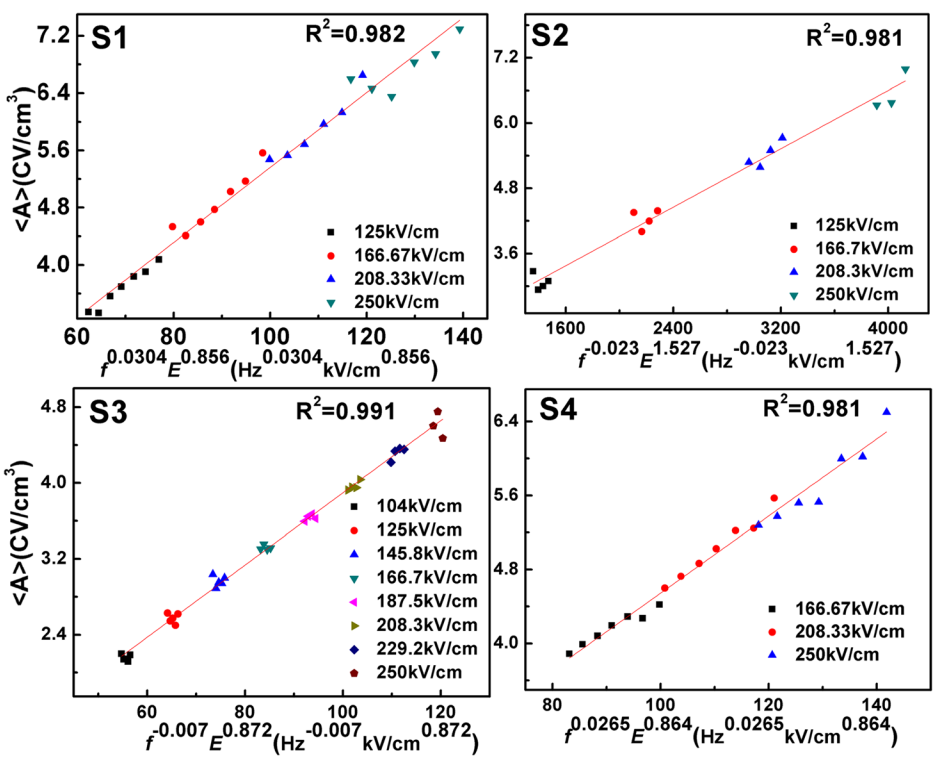

FIG. 5. Scaling plots of hysteresis area $\langle A \rangle$ against E and f for the PZT thin films with different interface configurations.

bottom electrodes affect the scaling behavior slightly via influencing the orientation and level of space charge.

This work was supported by Key Basic Research Project (973 Program) (Grant No. 2012CB619406), the National Natural Science Foundation of China (Nos. 10974216, U0937603, 61371059, and 51302295), Natural Science Foundation of Shanghai City (No. 13ZR1445600) and international partnership project of Chinese Academy of Science.

[1]N. Wongdamnern, A. Ngamjarurojana, Y. Laosiritaworn, S. Ananta, and R. Yimnirun, J. Appl. Phys. **105**(4), 044109 (2009).
[2]Y. Y. Guo, T. Wei, Q. Y. He, and J. M. Liu, J. Phys.: Condens. Matter **21**(48), 485901 (2009).
[3]R. Yimnirun, S. Ananta, Y. Laosiritaworn, A. Ngamjarurojana, and S. Wongsaenmai, Ferroelectrics **358**, 885 (2007).
[4]M. Rao, H. R. Krishnamurthy, and R. Pandit, Phys. Rev. B **42**(1), 856 (1990).
[5]J. M. Liu, H. P. Li, C. K. Ong, and L. C. Lim, J. Appl. Phys. **86**(9), 5198 (1999).
[6]B. Pan, H. Yu, D. Wu, X. H. Zhou, and J. M. Liu, Appl. Phys. Lett. **83**(7), 1406 (2003).
[7]J. M. Liu, H. L. Chan, and C. L. Choy, Mater. Lett. **52**(3), 213 (2002).
[8]R. Yimnirun, R. Wongmaneerung, S. Wongsaenmai, A. Ngamjarurojana, S. Ananta, and Y. Laosiritaworn, Appl. Phys. Lett. **90**(11), 112908 (2007).
[9]R. Yimnirun, Y. Laosiritaworn, S. Wongsaenmai, and S. Ananta, Appl. Phys. Lett. **89**(16), 162901 (2006).
[10]G. Yu, X. F. Chen, F. Cao, G. S. Wang, and X. L. Dong, Solid State Commun. **150**(23–24), 1045 (2010).
[11]X. F. Chen, X. L. Dong, H. L. Zhang, G. Yu, F. Cao, and G. S. Wang, Solid State Commun. **150**(15–16), 720 (2010).
[12]X. F. Chen, X. L. Dong, N. B. Feng, H. C. Nie, F. Cao, G. S. Wang, Y. Gu, and H. L. He, Solid State Commun. **149**(17–18), 663 (2009).
[13]D. W. Cao, H. Zhang, L. Fang, W. Dong, F. G. Zheng, and M. R. Shen, Appl. Phys. Lett. **97**(10), 102104 (2010).
[14]F. Chen, X. L. Tan, Z. Huang, X. F. Xuan, and W. B. Wu, Appl. Phys. Lett. **96**(26), 262902 (2010).
[15]J. Choi, J. S. Kim, I. Hwang, S. Hong, I. S. Byun, S. W. Lee, S. O. Kang, and B. H. Park, Appl. Phys. Lett. **96**(26), 262113 (2010).
[16]X. J. Meng, J. L. Sun, J. Yu, L. X. Bo, C. P. Jiang, Q. Sun, S. L. Guo, and J. H. Chu, Appl. Phys. Lett. **78**(17), 2548 (2001).
[17]N. Sama, R. Herdier, D. Jenkins, C. Soyer, D. Rémiens, M. Detalle, and R. Bouregba, J. Cryst. Growth **310**(14), 3299 (2008).
[18]J. Karthik, A. R. Damodaran, and L. W. Martin, Adv. Mater. **24**(12), 1610 (2012).
[19]F. Chen, Q. Z. Liu, H. F. Wang, F. H. Zhang, and W. B. Wu, Appl. Phys. Lett. **90**(19), 192907 (2007).
[20]X. F. Du and I. W. Chen, J. Appl. Phys. **83**(12), 7789 (1998).
[21]L. Yang, G. Wang, C. Mao, Y. Zhang, R. Liang, C. Soyer, D. Remiens, and X. Dong, J. Cryst. Growth **311**, 4241 (2009).
[22]Y. C. Zhang, C. J. Lu, Z. Z. Yang, W. N. Ye, and L. H. Xia, J. Appl. Phys. **111**(8), 084104 (2012).
[23]R. Bouregba, N. Sama, C. Soyer, G. Poullain, and D. Remiens, J. Appl. Phys. **107**(10), 104102 (2010).